Supporting Information

Graphene Nanochannels for Label-Free Protein Detection and Protein-Protein Interaction Analysis

Yangjun Cui[1], Long Gao[1], Cuifeng Ying[2]*, Jianguo Tian[1,3]*, Zhibo Liu[1,3,4]*

[1] *The Key Laboratory of Weak Light Nonlinear Photonics, Ministry of Education, School of Physics and Teda Applied Physics Institute, Renewable Energy Conversion and Storage Center, Nankai University, Tianjin 300071, China*

[2] *Advanced Optics & Photonics Laboratory, Department of Engineering, School of Science & Technology, Nottingham Trent University, Nottingham NG11 8NS, UK*

[3] *State Key Laboratory of Photovoltaic Materials and Cells, Nankai University, Tianjin 300071, China*

[4] *The Collaborative Innovation Center of Extreme Optics, Shanxi University, Taiyuan, Shanxi 030006, China*

*To whom correspondence should be addressed: E-mail, liuzb@nankai.edu.cn, jjtian@nankai.edu.cn, cuifeng.ying@ntu.ac.uk

S1 The relationship of pulses to volume and charge

When the contributions of slip and electroosmosis in the channel are ignored, the initial conductance G_0 in the channel is:[1, 2]

$$G_0 = \frac{w \cdot h}{L_{channel}}\left((\mu_k + \mu_{cl})n_{KCl}e + \frac{2 \cdot \mu_k \sigma}{h}\right) \quad (s1)$$

where $w, h, L_{channel}$ represents the width, height and length of the channel, n_{KCl} is the number density of K^+ or Cl^-, e is the elementary charge, σ is the surface charge density in the channel, and μ_k and μ_{cl} are the electrophoretic mobilities of K^+ and Cl^-. G_0 determines the baseline height of the current trajectory.

Proteins have complex shapes and structures, and their charge distribution is extremely complex. Some common protein shapes are often simplified to spherical, pie, or elliptic shapes. To simplify the calculation, we use the cylindrical protein structure and uniformly distributed surface charge to analyze the decrease in ionic conductance caused by its spatial repulsion ($G_{protein-repulsion}$) and the increase in conductivity caused by the introduction of protein charge into ions ($G_{protein-charge}$):

$$G_{protein-repulsion} = \frac{1}{L_{protein}}\left(-\frac{\pi}{4}d_{protein}^2(\mu_k + \mu_{cl})n_{kcl}e\right) \quad (s2)$$

$$G_{protein-charge} = \mu_k^* q_{protein}^* \quad (s3)$$

where $L_{protein}$ is the length of the protein, $d_{protein}$ is the diameter of the protein, μ_k^* is the effective electrophoretic mobility of K^+ moving along the protein, and $q_{protein}^*$ is the effective charge on the protein per unit length, which is assumed to be constant. So, the change in conductance ΔG is:

$$\Delta G = G_{protein-repulsion} + G_{protein-charge} \quad (s4)$$

S2 The relationship between the capture frequency and the applied voltage

We use the trapping probability model of the pore to analyze the trapping probability of the channel as a function of voltage. Mayro et al. concluded that the frequency f_e at which the protein enters the pore is:[3]

$$f_e = 2\pi C_0 r_e^3 \frac{k_B T}{h} \exp\left[\varphi(r_e) - \frac{\Delta G_0}{k_B T} + \frac{U}{k_B T}\right] \quad (s5)$$

where C_0 is the protein concentration, r_e is the entrance radius, k_B is the Boltzmann constant, h is the Planck constant, T is the absolute temperature, ΔG_0 is the free-energy barrier at equilibrium, U is the barrier reduction (or increase) due to electric. $\varphi(r_e)$ is the sum of the radial forces and the advection contribution, When the effects of protein moment of inertia and electroosmosis are ignored:

$$\varphi(r_e) = -\left[\frac{qI}{2\pi\sigma r_e}\right] \quad (s6)$$

$$I = -\frac{E}{2\pi\sigma {r_e}^2} \quad (s7)$$

where q is the protein charge, σ is the electrolyte conductivity, I is the ion current flowing through the pore, E is the electrical field. It can assume $U = k_B T\varphi(r_e)$, so

$$f_e = 2\pi C_0 r_e^3 \frac{k_B T}{h} \exp\left[2\varphi(r_e) - \frac{\Delta G_0}{k_B T}\right] \quad (s8)$$

The $\varphi(r_e)$ linearly increases with E, so when other coefficients are determined, the frequency and voltage of protein entering the channel should show a positive e-exponential growth trend:

$$f_e = A\exp(\alpha V) + \beta \quad (s9)$$

Where A, α is a parameter related to the channel structure and protein concentration, β is the fitting parameter, and V is the applied voltage.

S3 The molecular weight, $\Delta I/I_0$, number of charges carried (pH 8.1) and size parameters of proteins.

The size of all proteins was approximated using the ellipsoid model.[4] Based on the provided volume and length-to-diameter ratio, we can estimate the size of this equivalent ellipsoid.[4] It should be noted that although the ellipsoid approximation model fits well with the shapes of most proteins, for proteins with complex structures such as BSA, IgG, and IgM, which significantly deviate from perfect ellipsoids, this simple model has limitations. Even so, even for these proteins, their actual molecular shapes are closer to the ellipsoid approximation model than to perfect spheres.

Protein	Molecular weight (kDa)	$\Delta I/I_0$ (median)	Number of charges (e)	Size parameters[4] (length × width × height)
Streptavidin	65	0.00379	-2.4	6.9 nm × 6.9 nm × 6.4 nm
BSA	66.4	0.0063	-24.1	8.6 nm × 8.6 nm × 5.1 nm
GA-Rab-IgG	150	0.0084	-16.2	10.5 nm × 10.5 nm × 4.2 nm
Rab-IgG	150	0.00723	-16.2	10.5 nm × 10.5 nm × 4.2 nm
IgM	900	0.0109	-130	17.4 nm × 17.4 nm × 6.8 nm

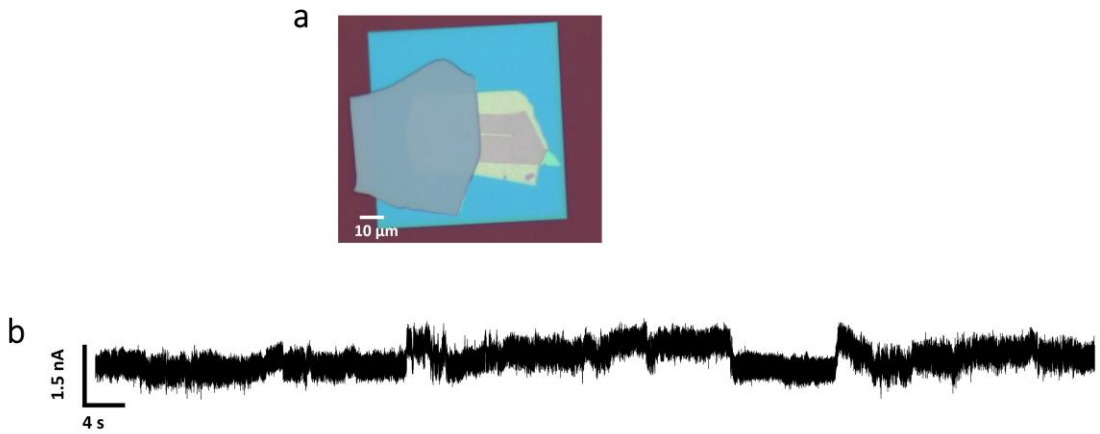

Figure S1. a) Diagram of a graphene channel sample with a height of 13 nm and a length of 5 μm. b) The current trajectory of BSA transmission in this channel.

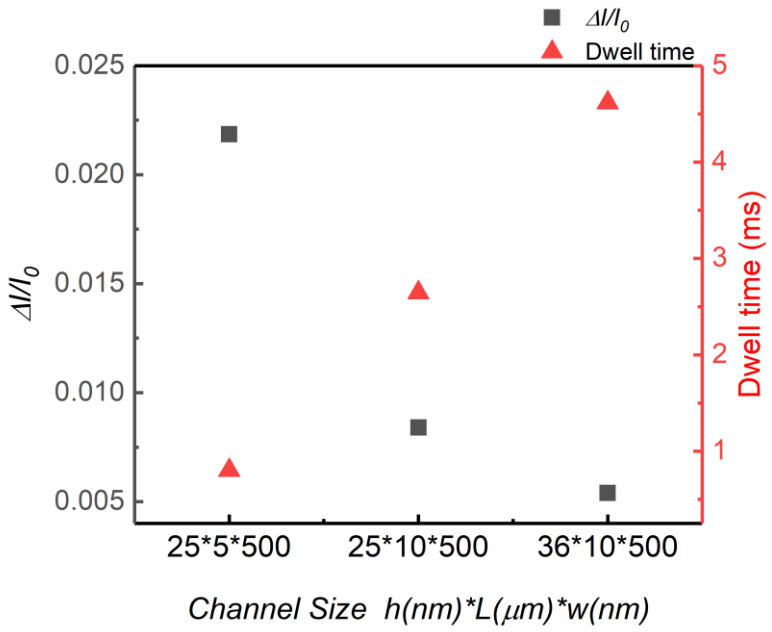

Figure S2. The dwell time and $\Delta I/I_0$ of GA-Rab-IgG transmission in three channels of different sizes.

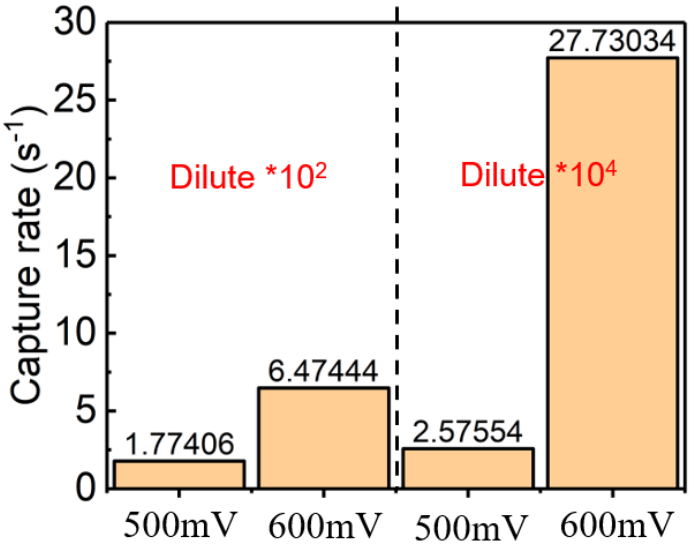

Figure S3. The capture rate of GA-Rab-IgG by the channel (h=36 nm, L=10 μm, w=500 nm) under two dilution conditions.

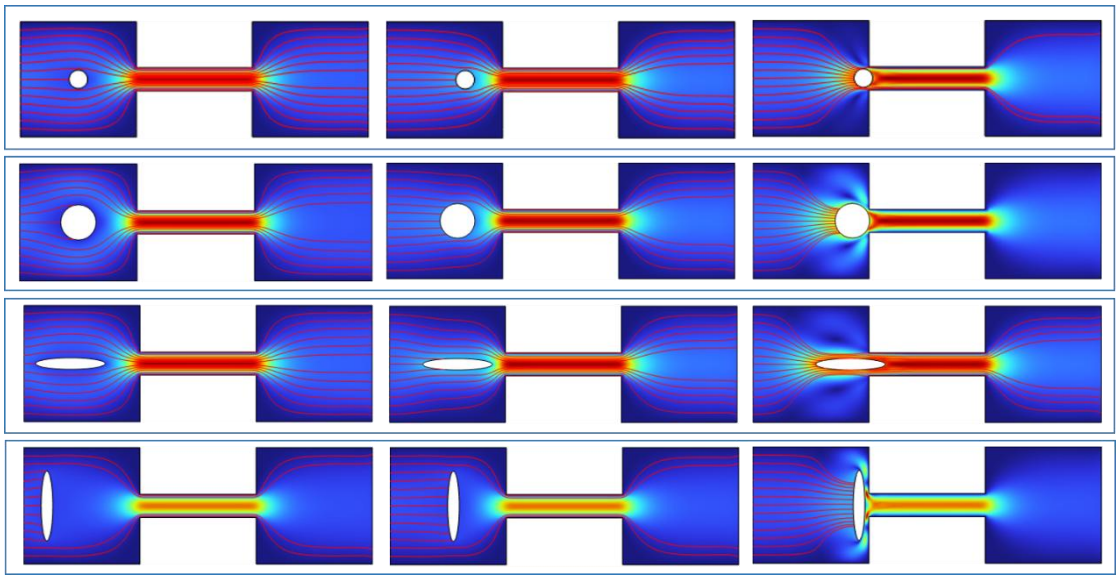

Figure S4. The transmission states of different structural proteins at the entrance of the channel.

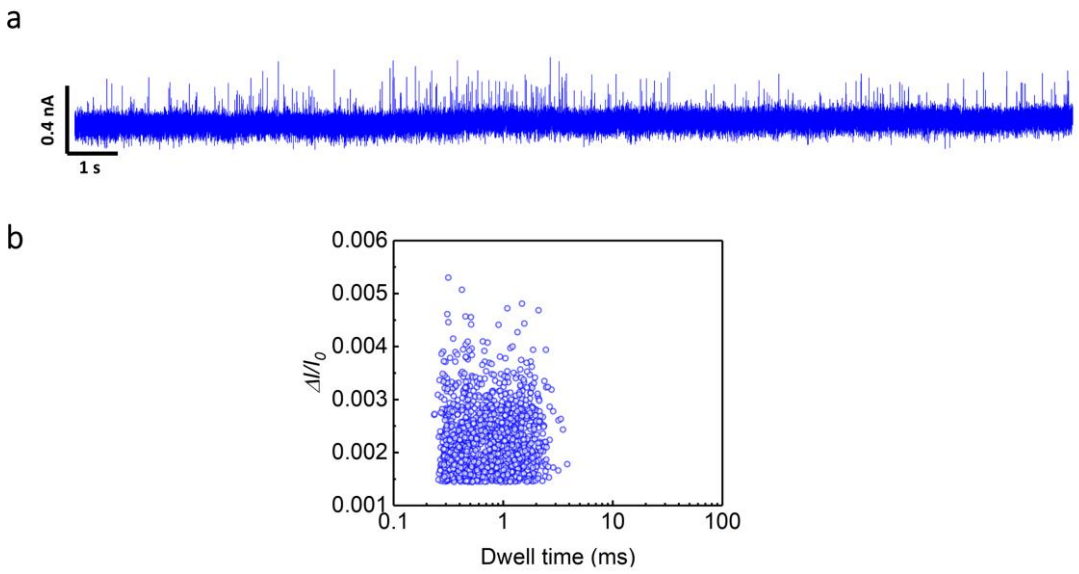

Figure S5. Transport experiment of protein marker. Its molecular weight is 30-209 kDa (30, 38, 50, 63, 70, 78, 105, 113, 154, 209), in in 1 M KCl, 5 mM Tris buffered at pH=8.1.

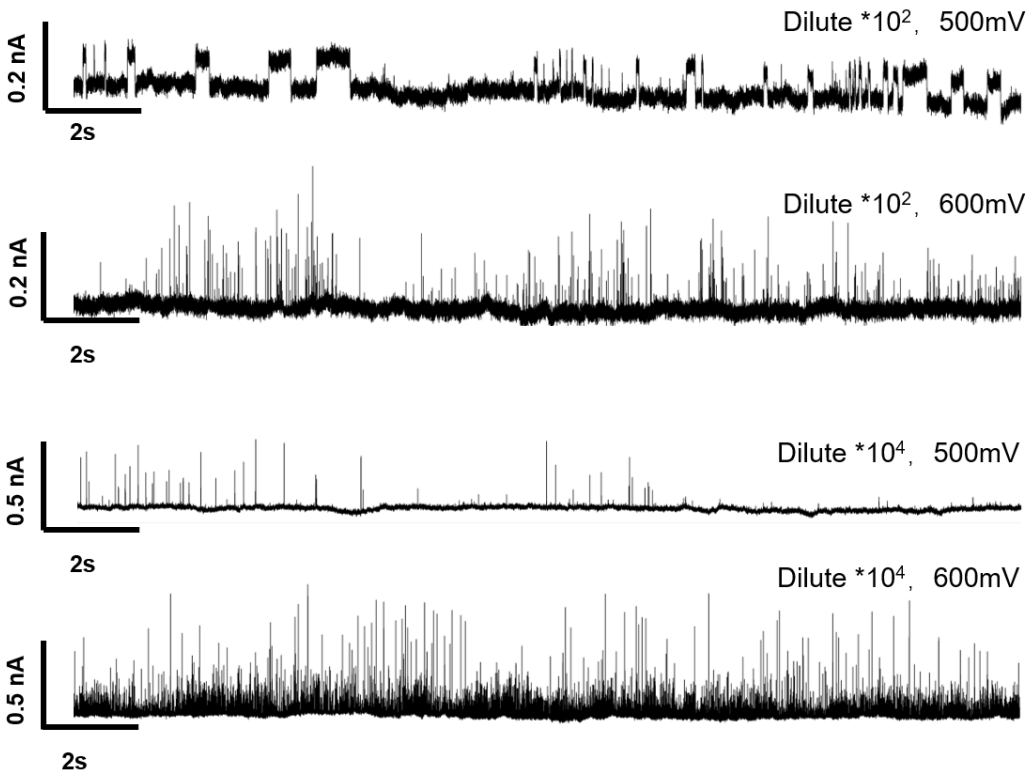

Figure S6. The current trace of GA-Rab-IgG by the channel (h=36 nm, L=10 μm, w=500 nm) under two dilution conditions.

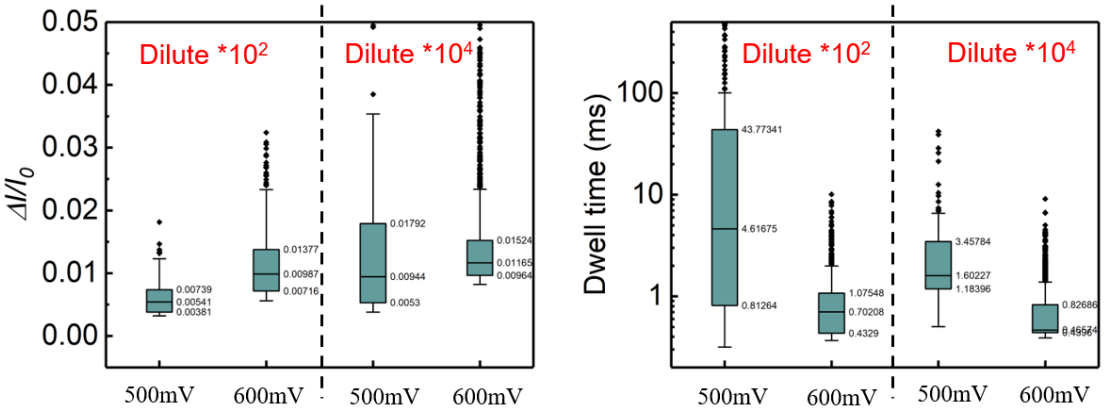

Figure S7. The Statistics on $\Delta I/I_0$ and dwell time for GA-Rab-IgG by the channel (h=36 nm, L=10 μm, w=500 nm) under two dilution conditions.

Reference

1. Smeets, R. M. M.; Keyser, U. F.; Krapf, D.; Wu, M. Y.; Dekker, N. H.; Dekker, C., Salt dependence of ion transport and DNA translocation through solid-state nanopores. *Nano Letters* **2006,** *6* (1), 89-95.

2. Goyal, G.; Freedman, K. J.; Kim, M. J., Gold nanoparticle translocation dynamics and electrical detection of single particle diffusion using solid-state nanopores. *Anal Chem* **2013,** *85* (17), 8180-7.

3. Chinappi, M.; Yamaji, M.; Kawano, R.; Cecconi, F., Analytical Model for Particle Capture in Nanopores Elucidates Competition among Electrophoresis, Electroosmosis, and Dielectrophoresis. *ACS Nano* **2020,** *14* (11), 15816-15828.

4. Houghtaling, J.; Ying, C.; Eggenberger, O. M.; Fennouri, A.; Nandivada, S.; Acharjee, M.; Li, J.; Hall, A. R.; Mayer, M., Estimation of Shape, Volume, and Dipole Moment of Individual Proteins Freely Transiting a Synthetic Nanopore. *ACS Nano* **2019,** *13* (5), 5231-5242.